CHAPTER 165

COUPLING OF A QUASI-3D MODEL FOR THE TRANSPORT WITH A QUASI-3D MODEL FOR THE WAVE INDUCED FLOW

Irene Katopodi[1], Nikos Kitou[1] and Huib J. de Vriend[2]

ABSTRACT

In this paper the coupling of a quasi-3D model for the suspended sediment transport with a quasi-3d model for the wave driven flow is presented. The quasi-3d model for the transport is based on an asymptotic solution of the wave-averaged convection-diffusion equation while the quasi-3D wave driven current model is based on a profile function technique. The resulting model is a low cost but detailed alternative to a full 3D model. An application is presented concerning cross-shore transport. Preliminary conclusions are drawn.

1. INTRODUCTION

The prediction of suspended sediment transport and subsequently of bed evolution in coastal areas is of vital importance for the operation and maintenance of engineering works. Numerical models are expected to play an increasingly significant role as a design and decision tool of the coastal engineer.

A variety of models have been presented in the literature with various degrees of sophistication as far as the constituent models are concerned. The present model involves two basic submodels of the same degree of sophistication: Both wave induced currents and suspended sediment transport are computed using quasi-3D techniques that exhibit the low computational cost of the 2DH models while at the same time provide information about the vertical structure of the flow and the suspended sediment concentration.

Moreover, in cross-shore flows local equilibrium is

---

1 Democritus University of Thrace, Department of Civil Engineering, 67100 Xanthi, Greece.
2 Delft Hydraulics, P.O. Box 152, 8300 AD, Emmeloord, the Netherlands.

assumed for the suspended sediment and as a result suspended sediment transport formulae are widely used for the calculation of the bed-level changes. Herein, in a cross-shore case the full convection-diffusion equation has been used.

2. THE QUASI-3D MODEL FOR THE SUSPENDED SEDIMENT TRANSPORT (LOG VELOCITY PROFILE)

The present work is an extension of the suspended sediment transport model presented by Katopodi and Ribberink (1990, 1992). A short description of the model follows:

The model is based on an asymptotic solution of the wave-averaged 3D convection-diffusion equation. The asymptotic solution was developed by Galappatti and Vreugdenhil (1985) for unidirectional flow under certain scale considerations. In the quasi-3D model for currents and waves the wave influence is included through a suitable modification of the vertical mixing coefficient and through the near-bed boundary condition (van Rijn, 1986). Two bed boundary conditions are used: Either the sediment concentration ("concentration" b.c.) or its vertical gradient at the near-bed reference level ("gradient" b.c) is assumed to adapt immediately to equilibrium conditions and are given as functions of local hydraulic and sediment parameters (for expressions see van Rijn, 1986).

Under the assumption that the velocity is described by $u(\mathbf{x},\zeta,t) = \bar{u}(\mathbf{x},t)\ p(\zeta)$ and $v(\mathbf{x},\zeta,t) = \bar{v}(\mathbf{x},t)\ p(\zeta)$ (one logarithmic component only) and the use of the "concentration" bed boundary condition the depth averaged equation reads:

$$\bar{c}_e = \bar{c} + \frac{\gamma_{21}}{\gamma_{11}}\frac{h}{w_s}\frac{\partial\bar{c}}{\partial t} + \frac{\gamma_{22}}{\gamma_{11}}\frac{h\bar{u}}{w_s}\frac{\partial\bar{c}}{\partial x} + \frac{\gamma_{22}}{\gamma_{11}}\frac{h\bar{v}}{w_s}\frac{\partial\bar{c}}{\partial y} -$$

$$- \frac{\gamma_{21}}{\gamma_{11}}\frac{h}{w_s}\frac{\partial}{\partial x}\left(\varepsilon_x\frac{\partial\bar{c}}{\partial x}\right) - \frac{\gamma_{21}}{\gamma_{11}}\frac{h}{w_s}\frac{\partial}{\partial y}\left(\varepsilon_y\frac{\partial\bar{c}}{\partial y}\right) \qquad (1)$$

where $\bar{c}$ and $\bar{c}_e$ are the depth averaged concentration and equilibrium concentration, $\bar{u}$ and $\bar{v}$ depth averaged velocities, h the water depth, the sediment fall velocity is w_s and γ_{ij} coefficients that depend only on the explicit knowledge of the vertical mixing coefficient, the fall velocity and the normalized velocity profile $p(\zeta)$ and can be computed in advance.After equation (1) has been solved for $\bar{c}$, the vertical concentration profile can be constructed in terms of already known profile functions (see Katopodi and Ribberink, 1992).

Equation (1) can be written as:

$$\bar{c}_e = \bar{c} + T_A \frac{\partial \bar{c}}{\partial t} + L_x \frac{\partial \bar{c}}{\partial x} + L_y \frac{\partial \bar{c}}{\partial y} - T_A \left(\frac{\partial}{\partial x}(\varepsilon_x \frac{\partial \bar{c}}{\partial x}) + \frac{\partial}{\partial y}(\varepsilon_y \frac{\partial \bar{c}}{\partial y}) \right) \tag{2}$$

with

$$T_A = \frac{\gamma_{21}}{\gamma_{11}} \frac{h}{w_s} , \quad L_x = \frac{\gamma_{22}}{\gamma_{11}} \frac{\bar{u}h}{w_s} , \quad L_y = \frac{\gamma_{22}}{\gamma_{11}} \frac{\bar{v}h}{w_s} \tag{3}$$

Equation (2) describes the adjustment of the depth-averaged concentration to its equilibrium value. The parameters T_A, L_x and L_y represent the characteristic scales in time and space of this adjustment process (adaptation time, adaptation lengths). If the "gradient" bed boundary condition is used, only the expressions for the adaptation time and length change in equation (3), (see Katopodi and Ribberink, 1992).

3. THE QUASI-3D MODEL FOR THE WAVE INDUCED FLOW

In (1) the velocity profile was assumed logarithmic which is not realistic in the wave driven nearshore circulation. Instead, the quasi-3D model for nearshore currents presented by de Vriend and Stive (1987) as modified by de Vriend and Ribberink (1988) is employed in this work (DVS in the following). This model is based in a profile function technique combined with a 2DH current formulation. The current is divided into a primary component and a number of secondary components due to the vertical nonuniformities of the various driving forces. The velocity is given as a similarity series:

$$u(x,\zeta,t) = \sum_{i=1}^{n} \bar{u}_i(x,t)\ p_i(\zeta) \tag{4a}$$

$$v(x,\zeta,t) = \sum_{i=1}^{n} \bar{v}_i(x,t)\ p_i(\zeta) \tag{4b}$$

where $\bar{u}_1$, $\bar{v}_1$ are depth averaged primary current, $\bar{u}_i$, $\bar{v}_i$ depth invariant parameters representing secondary current intensity, ζ=z/h and $p_i(\zeta)$ profile functions with:

$$\int_o^1 p_1(\zeta)d\zeta = 1 \quad \text{and} \quad \int_o^1 p_i(\zeta)d\zeta = 0 \quad \text{for } i > 1 \tag{5}$$

Equations (5) imply that the depth averaged flow is entirely determined by the primary current. The model consists of a depth-averaged wave-driven current module (see application, chapter 5) and the velocity profile extraction part.

In the DVS model complete description of the undertow and the boundary layer streaming is included. The model though is written in a general way so that secondary flows other than those due to waves (like Coriolis induced or wind induced flows) can easily be included.

The wave induced secondary velocity is consisting of a number of components due to various driving forces:

$$u_s(\zeta) = u_2(\zeta) + u_3(\zeta) + u_4(\zeta) + u_5(\zeta)$$

$$= \bar{u}_2\ p_2(\zeta) + \bar{u}_3\ p_3(\zeta) + \bar{u}_3\ p_3(\zeta) + \bar{u}_4 p_4(\zeta) \qquad (6)$$

where

$u_2(\zeta)$ secondary current due to the surface shear stress

$u_3(\zeta)$ secondary current due to secondary bottom shear stress

$u_4(\zeta)$ near-bottom drift due to spatial variation of the orbital velocity

$u_5(\zeta)$ near-bottom drift due to the boundary layer.

For expressions for the secondary velocities the reader is referred to Ribberink and de Vriend (1989). In fig.1 the velocity and its components are shown at the cross section of the flume x=30 m (cf.example). Near the bottom the effect of the boundary layer is clear.

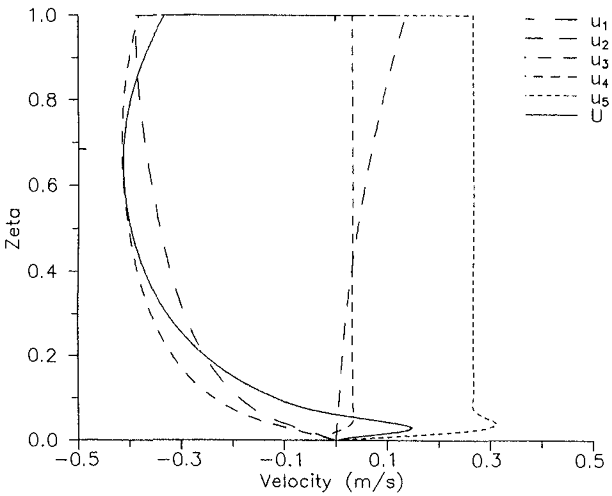

Fig.1 Current velocity and its components (x=30m)

4. COUPLING OF THE TWO QUASI-3D MODELS

In (1) the velocity was consisting of only one component (similarity was assumed). If the velocity is given as a similarity series, eq.(4), then equation (1) becomes:

$$\bar{c}_e = \bar{c} + \frac{\gamma_{21}}{\gamma_{11}} \frac{h}{w_s} \frac{\partial \bar{c}}{\partial t} +$$

$$+ \left(\sum_{i=1}^{n} \bar{u}_i \frac{\gamma_{22,i}}{\gamma_{11}} \right) \frac{h}{w_s} \frac{\partial \bar{c}}{\partial x} + \left(\sum_{i=1}^{n} \bar{v}_i \frac{\gamma_{22,i}}{\gamma_{11}} \right) \frac{h}{w_s} \frac{\partial \bar{c}}{\partial y}$$

$$+ \left(\beta \frac{\gamma_{23}}{\gamma_{11}} + \frac{\gamma_{24}}{\gamma_{11}} \right) \frac{1}{1+\beta} \frac{\partial z_s}{\partial t} \frac{1}{w_s} \bar{c}$$

$$+ \sum_{i=1}^{n} \left(\frac{\partial}{\partial x} (\bar{u}_i h) \frac{\gamma_{25,i}}{\gamma_{11}} \right) \frac{1}{w_s} \bar{c}$$

$$+ \sum_{i=1}^{n} \left(\frac{\partial}{\partial y} (\bar{v}_i h) \frac{\gamma_{25,i}}{\gamma_{11}} \right) \frac{1}{w_s} \bar{c}$$

$$- \frac{\gamma_{21}}{\gamma_{11}} \frac{h}{w_s} \left(\frac{\partial}{\partial x} \left(\varepsilon_x \frac{\partial \bar{c}}{\partial x} \right) + \frac{\partial}{\partial y} \left(\varepsilon_y \frac{\partial \bar{c}}{\partial y} \right) \right) \tag{7}$$

where β is the reference level normalized by the depth.

New terms have been added to the RHS of eq.(7), compared to eq.(1): The third and fourth term are now sums of similar terms due to the separate velocity components. The fifth term arises from the vertical transformation. The sixth and seventh terms are due to the vertical velocities that are computed via the continuity equation.

The above equation can be written in a more convenient form, similar to equation (2):

$$\bar{c}_e = (1 + V_T + V_x + V_y)\bar{c} + T_A \frac{\partial \bar{c}}{\partial t} + L_x \frac{\partial \bar{c}}{\partial x} + L_y \frac{\partial \bar{c}}{\partial y}$$

$$- T_A \left(\frac{\partial}{\partial x} \left(\varepsilon_x \frac{\partial \bar{c}}{\partial x} \right) + \frac{\partial}{\partial y} \left(\varepsilon_y \frac{\partial \bar{c}}{\partial y} \right) \right) \tag{8}$$

with

$$T_A = \frac{\gamma_{21}}{\gamma_{11}} \frac{h}{w_s}$$

$$L_x = \left(\sum_{i=1}^{n} \bar{u}_i \frac{\gamma_{22,i}}{\gamma_{11}} \right) \frac{h}{w_s} \qquad L_y = \left(\sum_{i=1}^{n} \bar{v}_i \frac{\gamma_{22,i}}{\gamma_{11}} \right) \frac{h}{w_s}$$

$$V_T = \left(\beta \frac{\gamma_{23}}{\gamma_{11}} + \frac{\gamma_{24}}{\gamma_{11}} \right) \frac{1}{1+\beta} \frac{\partial z_s}{\partial t} \frac{1}{w_s}$$

$$V_x = \sum_{i=1}^{n} \left(\frac{\partial}{\partial x} (\bar{u}_i h) \frac{\gamma_{25,i}}{\gamma_{11}} \right) \frac{1}{w_s}$$

$$V_y = \sum_{i=1}^{n} \left(\frac{\partial}{\partial y} (\bar{v}_i h) \frac{\gamma_{25,i}}{\gamma_{11}} \right) \frac{1}{w_s} \tag{9}$$

After (7), or (8), is solved for the depth-averaged concentration, the concentration profile can be constructed in terms of already known profile functions.

If "gradient" bed boundary condition is used only the expressions in (9) are different.

Although the number of coefficients to be computed in equation (7), or (8), has now increased significantly compared to (1), or (2), the time required for their computation keeps the model at operational level.

5. APPLICATION

The model described in the previous section was applied for a cross-shore case with field and wave data taken from the experiment conducted in the Hannover Big Wave Flume (Dette and Uliczka, 1986) in order to study the beach profile evolution due to the wave action at prototype scale. This experiment was used for intercomparison of profile models under the MAST-G6 Morphodynamics programme (Hedegaard et al, 1992). The waves were monochromatic (H= 1.5m T = 6s) and the wave propagation direction normal to the shore (bed configuration fig.2a).

In the present computation no wave-current interaction was included, the wave field was stationary and the steady-state current was computed. The steps followed are described below:

1. The wave heights (fig.2a) were computed with the use of the energy equation. Dissipation due to breaking was calculated using the bore analogy (see description of UNIBEST in Hedegaard et al, 1992).

2. For depth-averaged current the 1D continuity and momentum equations were solved:

$$\frac{\partial(\bar{u}h)}{\partial x} + \frac{\partial}{\partial x}\left(\frac{M_x}{\rho}\right) = 0 \qquad \text{continuity} \tag{10}$$

with

$$M_x = \frac{E}{c}\left(1 + \frac{7h}{L} Q_b\right) \qquad (11)$$

where $\bar{u}$ is the depth-averaged current velocity, M_x the wave mass flux, E the wave energy, c the wave celerity, L the wave length, h the water depth, Qb fraction of breaking waves set equal to 1 for breaking waves and to 0 for non-breaking waves and ρ the water density. The second factor in the parenthesis is the roller contribution.

$$0 = -g\frac{\partial z_s}{\partial x} + \frac{1}{\rho h}\frac{D}{c} - \frac{\tau_{b,p}}{\rho h} \qquad \text{momentum} \qquad (12)$$

where z_s is the free surface, D the total wave energy dissipation (due to breaking and due to bed friction), $\tau_{b,p}$ primary bed shear stress given by de Vriend and Stive (1987) as function of the depth mean velocity, the eddy viscosity and the bottom roughness amplification factor. In fig.2b and fig.2c the bed configuration and set-up and the depth averaged (primary) velocity are shown along the flume.

3. The secondary velocities were calculated according to Ribberink and de Vriend (1989), and the velocity profiles were constructed (fig.3a). In fig.3b velocity profiles are also shown in more detail (note the vertical axis where the position of the cross-section along the flume is depicted).

4. The adaptation time T_A and length L_x (fig.4a and 4b) as well as the factor due to vertical velocities V_x and the depth-averaged value of $\bar{c}_e$ (fig.5a) were computed by a separate module before the calculation of $\bar{c}$. The term V_T is zero because the steady state is examined.

5. Equation (8), was solved with upstream (shore) condition imposed equilibrium concentration and downstream (offshore) condition zero second derivative of the concentration. For "gradient" bed boundary condition the expressions (9) are different. The value of the horizontal eddy viscosity (fig.4c) was given by:

$$\varepsilon_x = M\, h \left(\frac{D}{\rho}\right)^{1/3} \qquad (13)$$

where M is a coefficient of the order of one. The depth averaged concentration for the two bed boundary conditions is shown in fig.(5a).

6. The concentration profiles (fig.5b and 5c) were then constructed in terms of the depth averaged concentration and profile functions computed before .

7. Finally, the suspended sediment transport rate was

calculated using the following equation:

$$S_x = h \int_0^1 uc \, d\zeta - h \int_0^1 \epsilon_x \frac{\partial c}{\partial x} \, d\zeta \qquad (14)$$

In fig.6 the suspended sediment transport rate computed from equation (14) is plotted for "concentration" and for "gradient" boundary condition. In the same plot the suspended sediment transport rate under equilibrium conditions is also shown.

The results of the example are discussed in the following:

Considerable difference exists between the equilibrium concentration and the concentration computed from the convection-diffusion equation. This is shown in fig. (5a) as far as depth-averaged quantities are concerned for both boundary conditions. The difference is more important in cross section at x=40m where the equilibrium concentration is bigger and at cross section at x=50 m where the opposite happens. The peak of the concentration is more onshore for equilibrium conditions. In figures 5b, 5c (concentration profiles) the difference between the concentrations computed with the use of the two bed boundary conditions should be noticed, especially in the cross-section at 40m. The gradient bed boundary condition results in somewhat smoother concentration (result of the bigger adaptation length (see fig.4a). No definite conclusion on which boundary condition is appropriate can be drawn until comparison with measurements is made.

In fig.6 we can see that the non-equilibrium transport presents a discontinuity in cross-section at x=40m. This is due to the wave formulation we have chosen. In the computation of the wave mass-flux the roller term is added suddenly as soon as the waves start breaking and this causes a discontinuity in the depth averaged velocity. This discontinuity can be removed with an alternative formulation of the roller contribution to the wave mass flux. Inclusion of random waves will make even smoother the quantities involved. The discontinuity occurs in the first term of the RHS of (14) where the concentration is multiplied by the velocity.

Nevertheless, the horizontal gradients of the non-equilibrium transport are smaller than those of the equilibrium one and it is expected that the bar that will be formed will have more damped shape than the one computed if suspended sediment transport is assumed to be in equilibrium (as is implied in transport formulae).

In Katopodi and Ribberink (1990,1992) it was argued that when the space (time) computational grid size is smaller than the adaptation length (time) then the adaptation process (to equilibrium) should be described with the use of a non-equilibrium transport model

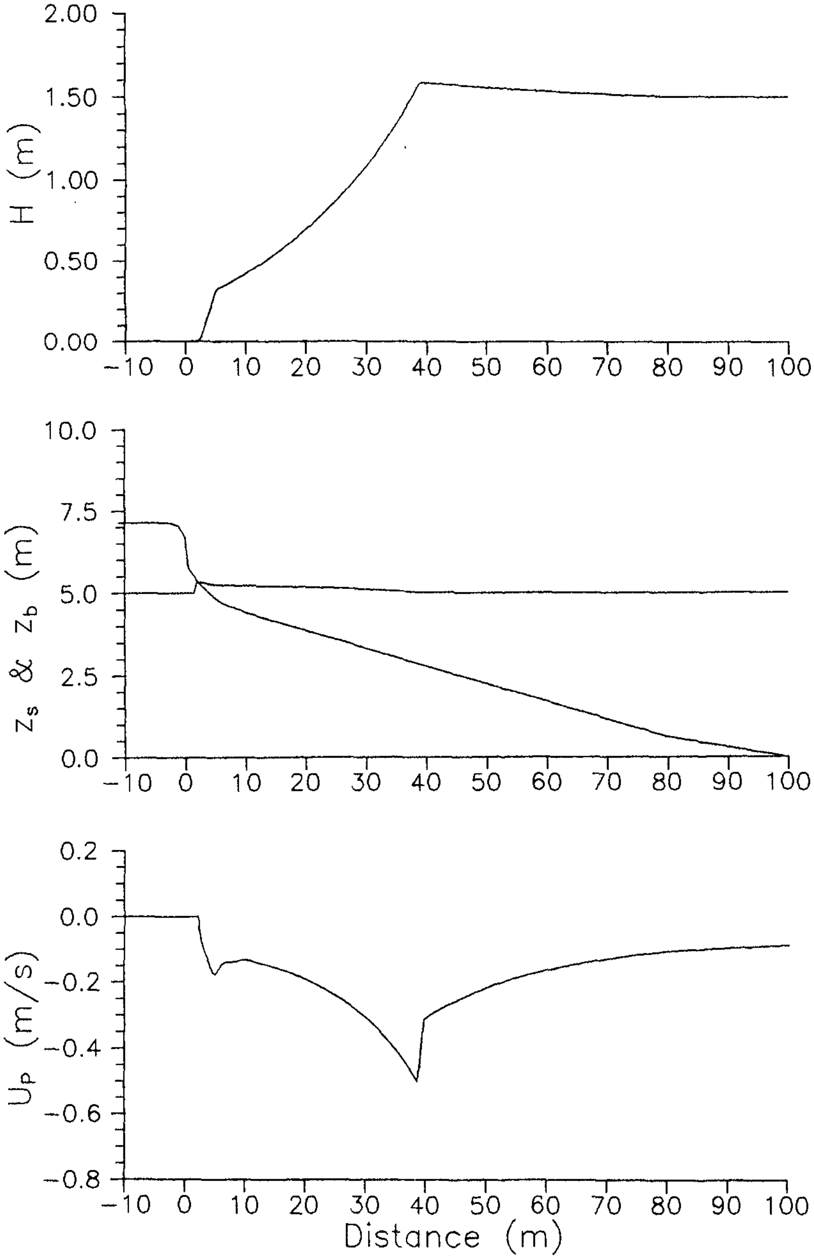

Fig.2 a) Wave height, b) Bed configuration and set-up
c) Depth-averaged (primary) velocity.

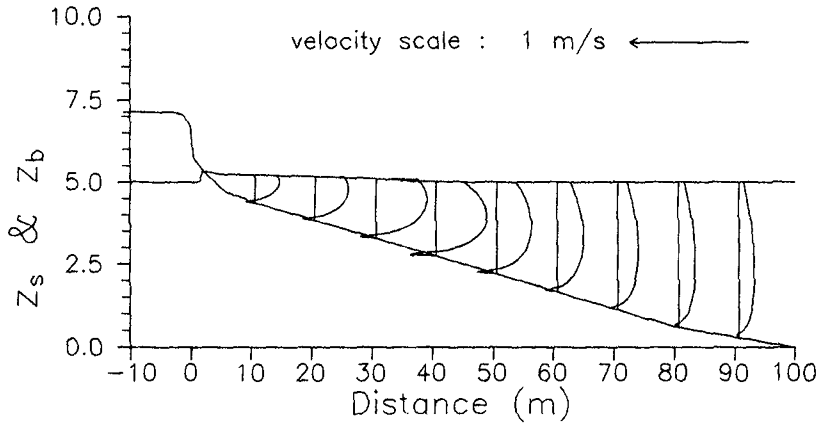

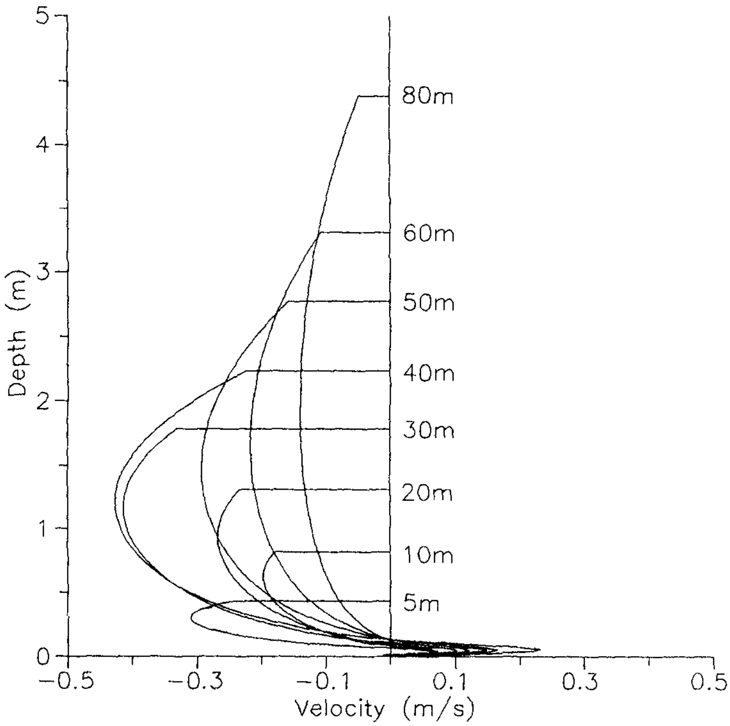

Fig.3 a) Velocity profiles along the flume,
b) Velocity profiles along the flume (detailed)

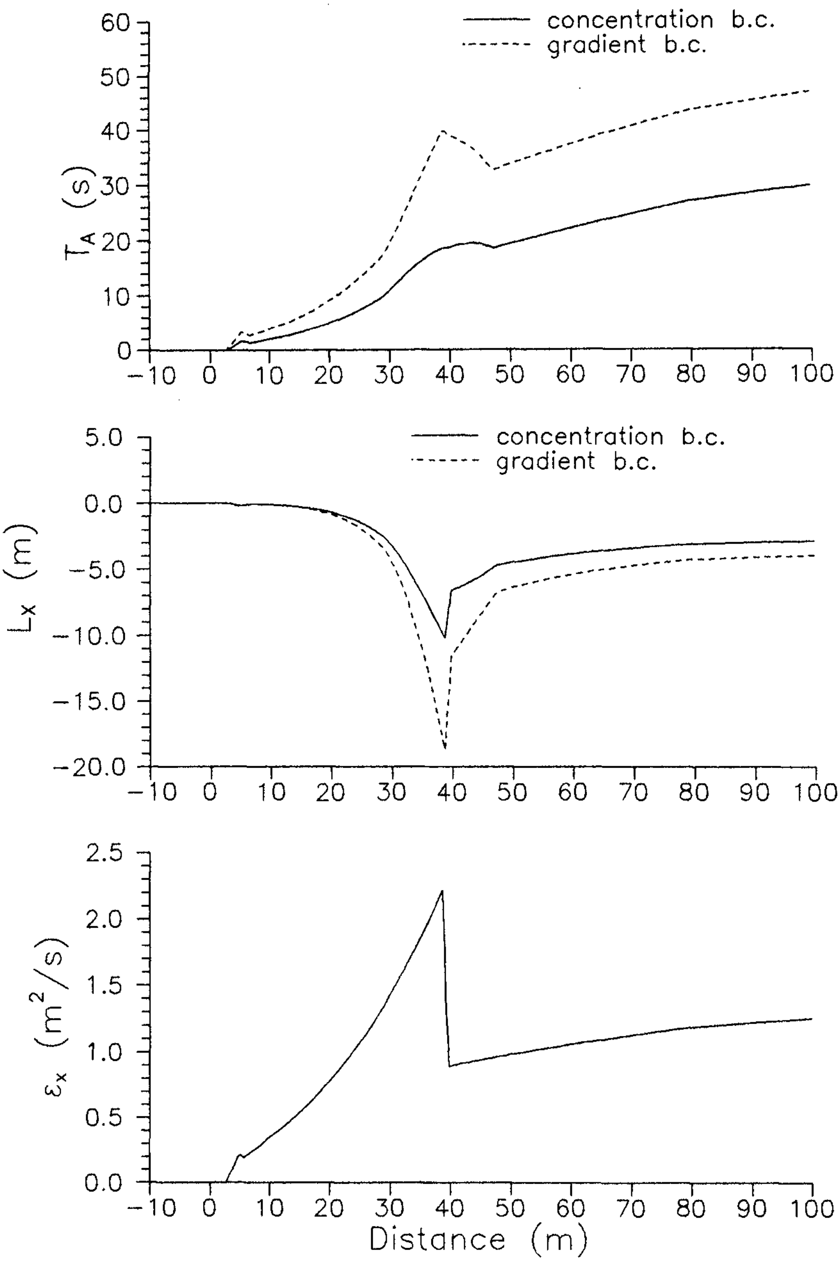

Fig.4 a) Adaptation time, b) Adaptation length
c) Horizontal eddy viscosity

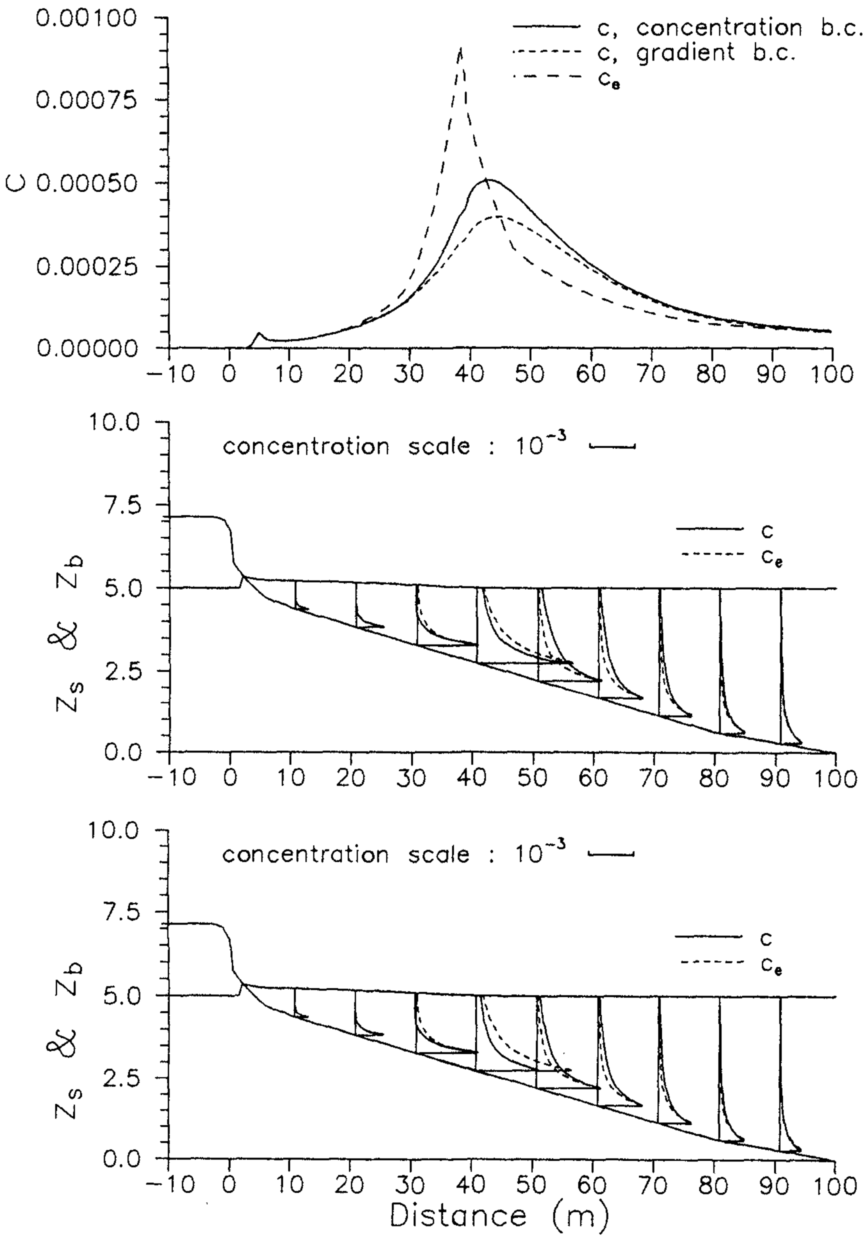

Fig.5 a) Depth-averaged concentration,
b) Concentration profiles ("concentration" bed bc)
c) Concentration profiles ("gradient" bed bc)

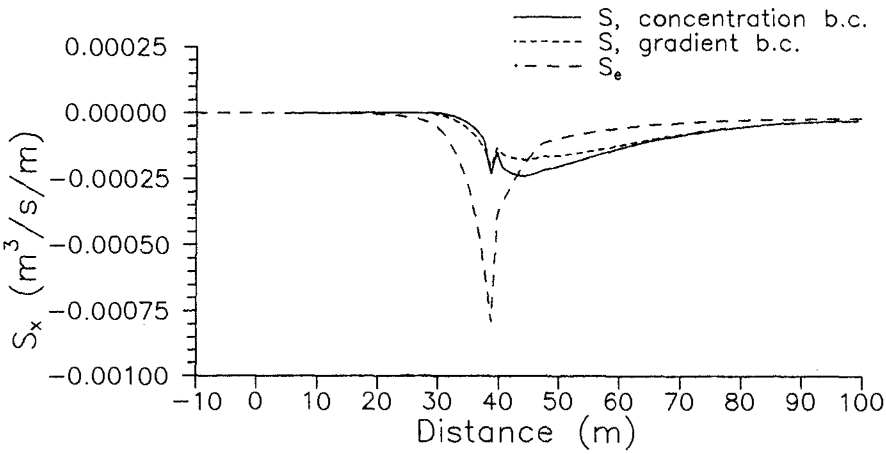

Fig.6 Suspended sediment transport rates

(convection-diffusion equation). Following the above reasoning, the importance of the non-equilibrium effects could be foreseen (before the solution of the convection diffusion equation) by comparison of the adaptation length (fig.4b) with the required computational space grid. In the experiment of Dette and Uliczka (1986) the bar has a width of about 10 m and a grid of about 0.5 m is required to describe it. The grid size is much smaller than the adaptation length in the biggest part of the flume, especially in the surf zone, and this indicates that non equilibrium effects should be taken into account in the transport computation. Of course, their impact on the bed-level changes should be shown quantitatively

6. CONCLUSIONS

A model for the suspended sediment transport is presented for wave induced flows. The current velocities are given as a (similarity) series of vertical profiles. The suspended sediment transport is computed with the use of a quasi-3d model of the convection diffusion equation. The effect of the vertical velocity that is computed via the continuity equation is included.

Although the number of coefficients to be computed before the solution of eq. (7) is much larger than when the velocity was consisting of a unique profile, the time required for their computation is very small compared to that of the actual solution of the equation.

Both current and transport modules require gradual changes in hydraulic conditions and are particularly suited for large computational areas.

This work is a first attempt to develop a sediment transport model and the effort has been put mostly at the technical part (formulation of the coupling). The Lagrangian and the wave asymmetry transport have not yet been included despite their importance. After the inclusion of the Lagrangian drift correction (as an additional profile), the wave asymmetry transport as well as bed load transport and bed slope effects, we will be able to reach more definite conclusions about the real magnitude and importance of the different phenomena on the sediment transport in the coastal zone.

ACKNOWLEDGMENT

This work was undertaken as part of the MAST G6 Coastal Morphodynamics research programme. It was funded by the Commission of the EC, Directorate General for Science, Research and Development, under MAST contract no. 0035-C.

APPENDIX I. REFERENCES

DETTE,H. and ULICZKA,K., 1986.
Velocity and sediment concentration fields across surf zone. Proc. 20th ICCE, Taipei, Taiwan.

DE VRIEND,H.J. and STIVE,M.J.F., 1987.
Quasi-3D modelling of nearshore currents. Coastal Engineering, Vol. 11.

DE VRIEND,H.J. and RIBBERINK,J., 1988.
A quasi-3D mathematical model of coastal morphology. Proc. 21st ICCE, Malaga, Spain.

GALAPPATTI,R. and VREUGDENHIL,C.B., 1985.
A depth integrated model for suspended sediment transport. J. Hydr. Res. Vol. 23, No. 4.

HEDEGAARD,I.B., ROELVINK,J.A., PECHON,P., NICKOLSON,J., and HAMM,L., 1992.
Intercomparison of coastal profile models. Proc., 23rd ICCE, Venice, Italy.

KATOPODI,I. and RIBBERINK,J.S., 1990.
A QUASI-3D model for suspended sediment transport by currents and waves. Proc. 22nd ICCE, Delft.

KATOPODI,I. and RIBBERINK,J.S.,1992.
Quasi-3D modelling of suspended sediment transport by currents and waves. Coastal Engineering, Vol 18.

RIBBERINK,J.S. and DE VRIEND,H.J., 1989.
VOORDELTA morphological study, Report H526, Delft Hydraulics.

RIJN,L.C. van, 1986.
Sedimentation of dredged channels by currents and waves. J. of Waterway Port Coastal and Ocean Eng.,Vol.112, No.5